

Entropy-Constrained Noise Yields Superdiffusive Dynamics in Axonal Growth

Julian Sutaria and Cristian Staii*

Department of Physics and Astronomy, Tufts University, Medford, MA, 02155, USA

(Dated: June 16, 2025)

We present a coarse-grained stochastic model for axonal extension on periodic arrays of parallel micropatterns that integrates three key biophysical mechanisms: (i) the molecular clutch that couples actin retrograde flow to substrate adhesions, (ii) an active biopolymer-based mechanism generating traction-force fluctuations, and (iii) the mechanical interaction of the growth cone with the micropatterned substrate. Using the Shannon–Jaynes maximum entropy principle with constraints derived from experimental observations, we derive a unique probability distribution for the colored acceleration noise that enters the Langevin equation. The resulting stationary process exhibits power-law temporal correlations with negative exponent $\alpha < 0$, which accounts for the observed superdiffusive dynamics of axons. For biologically relevant parameters the model predicts $\alpha = -1/2$, in close quantitative agreement with measurements of cortical neurons cultured on patterned substrates.

Introduction. Neurons are the fundamental information-processing units of the brain, consisting of a cell body, branched dendrites that receive signals, and long axons that transmit impulses to other cells [1–3]. Understanding how axons grow and self-organize into functional networks is a central problem in science, with broad implications for nonequilibrium dynamics, pattern formation, and the physical principles governing complex biological systems [4–8]. A major goal is to identify the minimal set of rules and physical variables that govern such directed cellular motion [8–12]. Although recent advances have characterized key aspects of cytoskeletal dynamics and adhesion, a quantitative framework that captures axonal motility remains incomplete [7, 13–15].

Engineered micropatterned substrates provide a powerful platform for probing axonal dynamics under well-controlled conditions, enabling direct connections between microscopic mechanisms and macroscopic growth behavior [16–20]. In previous work [21], we demonstrated that axons growing along periodic microfabricated patterns exhibit superdiffusive motion, with mean-squared displacement (MSD) scaling as $\langle \Delta x^2(t) \rangle \propto t^\nu$ over time scales of several tens of hours, where $\nu \simeq 1.4$. These results were obtained using cortical neurons cultured on poly-D-lysine-coated polydimethyl-siloxane (PDMS) substrates patterned with periodic parallel ridges separated by grooves [19–22] (Fig. 1). While existing mechanochemical models describe several important processes, such as actin polymerization, molecular clutch binding, and substrate interactions, they fail to capture this robust power law behavior due to the lack of a direct theoretical link between measurable inputs and a complete stochastic description of the driving forces [1, 7, 13].

In this Letter we show that Shannon information theory provides such a framework. By imposing only experimentally motivated constraints on the protrusive acceleration noise—stationarity, zero mean, and a finite mean adhesion lifetime—the Shannon–Jaynes Maximum En-

tropy (MaxEnt) principle selects the *unique* probability distribution consistent with these assumptions. Applying MaxEnt to a superposition of Ornstein–Uhlenbeck (OU) traction pulses yields a Gamma-distributed spectrum: $p(\lambda) \propto \lambda^{-(1+\alpha)} e^{-\beta\lambda}$, which produces a colored acceleration noise with autocorrelation $C_a(\tau) \propto |\tau|^\alpha$, where $\alpha < 0$. For biologically relevant parameters the model predicts $\alpha = -1/2$, quantitatively reproducing the observed superdiffusive scaling without adjustable parameters and revealing heavy-tailed force fluctuations as a direct outcome of minimum information constraints.

Molecular clutch and topographical feedback. Growth cones convert environmental signals into directed motion by coordinating cytoskeletal dynamics and cell-substrate adhesion through a molecular clutch mechanism [1–3, 13]. In this model, actin filaments polymerize at the leading edge (actin treadmilling), while myosin II motors pull actin filaments together and induce retrograde flow. Transmembrane adhesion receptors such as integrins and cadherins form point contacts (PCs) with the substrate, mechanically linking the actin network to the extracellular environment and modulating traction forces (Fig. 1(b)). Swanson and Wingreen demonstrated that active biopolymers such as actin filaments or microtubules can be modeled as ordered chains of bound subunits [24]. In the continuum limit, the distribution of polymer lifetimes exhibits a diffusive prefactor $t^{-3/2}$, imparting a heavy-tailed character to the dynamics. We propose that these long-lived filaments store elastic energy, which is intermittently released as traction forces exerted against the substrate. In addition, the micropattern topography imposes an effective linear spring with stiffness k_\perp , which suppresses lateral deviations while leaving longitudinal motion weakly damped [19, 20]. As a result, intermittent bursts of actin and microtubule polymerisation become synchronized through substrate-dependent traction regulation. The stochastic nature of these underlying processes generates a colored force noise that enters the coarse-grained Langevin de-

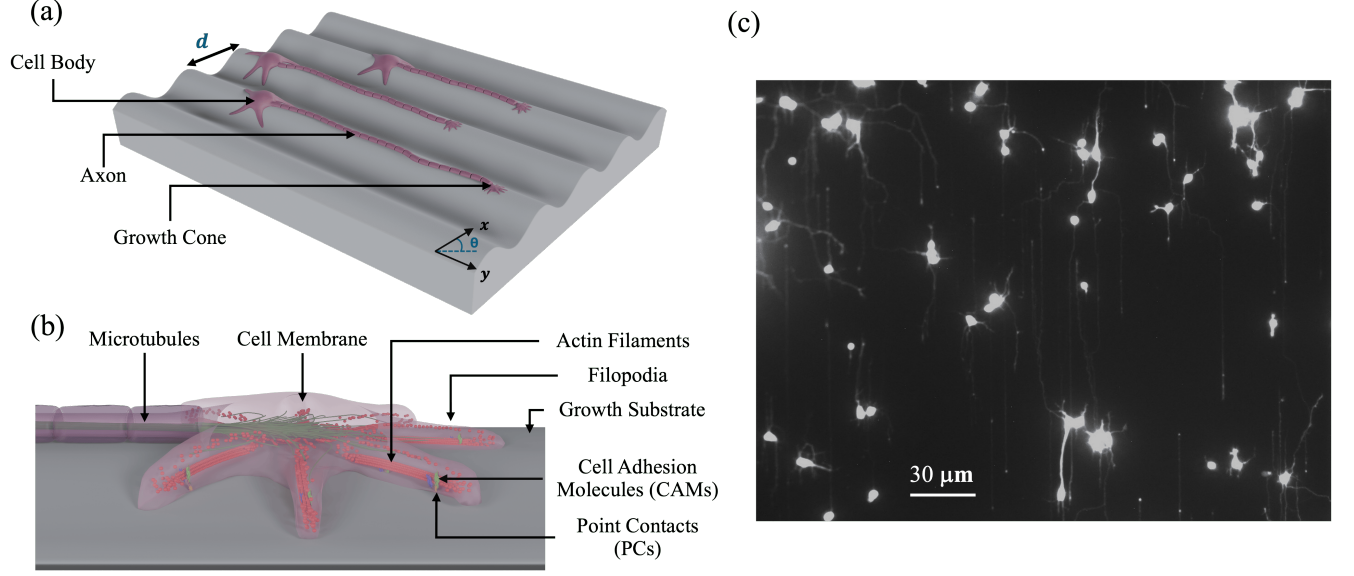


FIG. 1. (a) Schematic representation of a micropatterned PDMS surface. Periodic surface patterns are shown along the x direction, with spatial period d and uniform ridge height. The y -axis is oriented parallel to the PDMS grooves. Cortical neurons are cultured on the micropatterned substrate, extending a long axon aligned with the grooves and several shorter dendrites. Axonal extension is guided by the growth cone. The growth angle, $\theta(t)$, is defined as the angle between the axonal velocity and the x -axis at time t . (b) Schematic illustration of the growth cone and clutch mechanism, highlighting key cytoskeletal components. Interactions between cell adhesion molecules (integrins, cadherins) and actin filaments generate traction forces that drive forward motion of the growth cone. (c) Fluorescence images illustrating axonal growth for cortical neurons cultured on micropatterned PDMS substrates, with spatial period $d = 3\mu\text{m}$. The image shows strong axonal alignment along the direction of the micropatterns. Details on the fabrication of PDMS substrates and neuron culture are provided in the Supplemental Material [23].

scription of axonal extension $x(t)$:

$$\ddot{x} + \gamma \dot{x} = a(t), \quad (1)$$

with $\gamma > 0$ the damping constant, and $a(t)$ the net protrusive acceleration generated by cytoskeletal filaments.

Physical origin of $a(t)$. The clutch model posits that actin retrograde flow, with velocity v_r is coupled to nascent adhesions of lifetime τ_{adh} [13, 25]. Unbinding events transfer traction to the substrate, producing pulsatile forward displacements $\delta x \approx v_r \tau_{adh}$. This sequence of discrete traction pulses generates long-range correlated forces to the center of mass of the growth cone [26, 27]. Each adhesion stores elastic energy while bound and releases it upon detachment, producing an exponentially decaying force pulse that relaxes with rate $\lambda \simeq 1/\tau_{adh}$ [18, 27]. We therefore coarse-grain the biopolymer ensemble into a single effective relaxation rate λ that characterizes the traction-force mode it excites. Because adhesion events are independent and the Langevin equation is linear, the total acceleration can be expressed as a superposition of independent Ornstein–Uhlenbeck (OU) modes. As a result, we model the dynamics using a colored acceleration noise $a(t)$, which represents the aggregate effect of intermittent polymerization and traction

events:

$$a(t) = \int_0^\infty d\lambda \eta_\lambda(t), \quad \dot{\eta}_\lambda = -\lambda \eta_\lambda + \sqrt{2D_\lambda} \xi_\lambda(t), \quad (2)$$

where ξ_λ are independent gaussian noises. Each relaxation rate λ is drawn from a probability density $p(\lambda)$, to be derived from the MaxEnt principle below.

For an adhesion with lifetime $\tau_{adh} = 1/\lambda$, the traction amplitude of a single OU mode decays exponentially as $\eta_\lambda(t) = \eta_\lambda(0)e^{-\lambda t}$, with covariance $\langle \eta_\lambda(t) \eta_\lambda(t + \tau) \rangle = (D_\lambda/\lambda)e^{-\lambda|\tau|}$. Independence of the gaussian noises ξ_λ implies that covariances add linearly, so that the auto-correlation function for the total acceleration $a(t)$ is given by:

$$C_a(\tau) \equiv \langle a(t) a(t + \tau) \rangle = \int_0^\infty d\lambda \frac{D_\lambda}{\lambda} e^{-\lambda|\tau|}. \quad (3)$$

The clutch model imposes $D_\lambda/\lambda = \rho_a^2 p(\lambda)$, with ρ_a the variance of the distribution. Consequently $C_a(\tau)$ is proportional to the Laplace transform of $p(\lambda)$.

Maximum-entropy derivation of the probability density $p(\lambda)$. Building on the molecular clutch mechanism, the active biopolymer model of axonal growth, and the mechanical coupling between the axon and the micropatterned substrate, we use the maximum-entropy principle

to derive the probability distribution $p(\lambda)$ governing $a(t)$, and show that it naturally gives rise to power-law temporal correlations with a negative exponent.

The Shannon–Jaynes (MaxEnt) principle states that, among all candidate probability distributions $p(\lambda)$ consistent with a given set of constraints, the distribution that maximizes the entropy [28, 29]:

$$S[p] = - \int_0^\infty p(\lambda) \ln \frac{p(\lambda)}{m(\lambda)} d\lambda, \quad (4)$$

introduces the *least* additional bias beyond what is imposed by the known information. Here, $m(\lambda)$ represents a prior measure (or reference distribution) that encodes baseline knowledge in the absence of constraints.

To determine this distribution, we maximize the entropy in Equation (4) subject to two constraints: (1) normalization, $\int_0^\infty p(\lambda) d\lambda = 1$; and (2) a finite mean relaxation rate $\langle \lambda \rangle = \Lambda_1 \sim k_\perp / \zeta$, where Λ_1 is determined by the cell-substrate interactions through the effective lateral stiffness k_\perp and the viscous damping coefficient ζ , associated with motion perpendicular to the micropatterned grooves [20].

Introducing Lagrange multipliers (α, β) for the two constraints, and using a Jeffreys prior $m(\lambda) = \lambda^{-(1+\alpha)}$, chosen to promote exponentially decaying force pulses, we extremize the functional:

$$\mathcal{J}[p] = S[p] - \alpha \left(\int p - 1 \right) - \beta \left(\int \lambda p - \Lambda_1 \right). \quad (5)$$

Functional differentiation $\delta \mathcal{J} / \delta p = 0$ yields (see Supplemental Material [23]):

$$p(\lambda) = \frac{1}{Z} \lambda^{-(1+\alpha)} e^{-\beta \lambda}, \quad Z = \int_0^\infty \lambda^{-(1+\alpha)} e^{-\beta \lambda} d\lambda. \quad (6)$$

Note that the integral converges both at $\lambda \rightarrow 0^+$ and $\lambda \rightarrow \infty$ if $\beta > 0$ and $\alpha < 0$. Elementary Gamma-function algebra (refer to Supplemental Material [23]) yields:

$$Z = \beta^\alpha \Gamma(-\alpha). \quad (7)$$

The fixed mean $\langle \lambda \rangle$ determines the scale for the exponential cutoff β : $\langle \lambda \rangle = \frac{1}{Z} \int_0^\infty \lambda^{-\alpha} e^{-\beta \lambda} d\lambda \implies \beta = \frac{\Gamma(1-\alpha)}{\langle \lambda \rangle \Gamma(-\alpha)}$.

The acceleration autocorrelation at long times. Substituting the MaxEnt solution for $p(\lambda)$ (Equation (6)) into the Laplace transform for the acceleration autocorrelation function (Equation (3)), gives:

$$C_a(\tau) = \rho_a^2 \left(1 + \frac{|\tau|}{\beta} \right)^\alpha \xrightarrow{|\tau| \gg \beta} \sigma_a^2 |\tau|^\alpha. \quad (8)$$

with $\sigma_a^2 \equiv \rho_a^2 / \beta$.

Thus maximizing the Shannon–Jaynes entropy under the two experimental constraints yields a unique Gamma-type probability density $p(\lambda)$ for the colored acceleration

spectrum. The main effect of the clutch traction pulses is to generate a heavy-tailed distribution with exponent $-(1+\alpha)$ in Equation (6). This results in a power-law decay with a *negative* exponent $\alpha < 0$ in the acceleration autocorrelation function, while the exponential cutoff β encodes the finite lifetime of adhesions.

Superdiffusive growth of axons on micropatterned substrates. Using the clutch mechanism and the MaxEnt principle we have derived an explicit model for axonal growth. Next, we show that this model accounts for the experimentally observed superdiffusive dynamics of axons on micropatterned PDMS substrates. We start with the Langevin Equation (1) for growth cone position $x(t)$, where $a(t)$ is the stochastic acceleration with power-law autocorrelation for large times $\tau \gg \beta$:

$$\langle a(t) a(t+\tau) \rangle = \sigma_a^2 \tau^\alpha, \quad (9)$$

To find the position $x(t)$, we integrate Equation (1) twice to obtain the formal solution:

$$\begin{aligned} x(t) &= \int_0^t \left[\int_0^u e^{-\gamma(u-s)} a(s) ds \right] du \\ &= \frac{1}{\gamma} \int_0^t \left[1 - e^{-\gamma[t-s]} \right] a(s) ds. \end{aligned} \quad (10)$$

assuming zero initial velocity.

By using the power-law autocorrelation in Equation (9) and Equation (10) we get (Supplemental Material [23]):

$$\begin{aligned} \langle x^2(t) \rangle &= \\ \frac{\sigma_a^2}{\gamma^2} \int_0^t \int_0^t \left[1 - e^{-\gamma[t-s]} \right] \left[1 - e^{-\gamma[t-s']} \right] |s - s'|^\alpha ds ds'. \end{aligned} \quad (11)$$

This double integral completely specifies the mean-squared displacement (i.e. axonal mean squared length) $\langle x^2(t) \rangle$ at any finite t . For large times $t \gg 1/\gamma$ we obtain (Supplemental Material [23]):

$$\langle \Delta x^2(t) \rangle \simeq \frac{2\sigma_a^2}{\gamma^2} \frac{t^{2+\alpha}}{(1+\alpha)(2+\alpha)}. \quad (12)$$

The power-law growth, $\langle x^2(t) \rangle \propto t^{\alpha+2}$, indicates that the process can exhibit subdiffusion, superdiffusion, or normal diffusion, depending on the value of α . To determine this exponent, we build on the model of active biopolymers developed by Swanson and Wingreen, in which the joint probability distribution $p(x, L, t)$ —for the cap size x and filament length L —satisfies a Fokker–Planck equation with drift from polymerization and hydrolysis rates [24]. First-passage time (FPT) analysis yields a disassembly time distribution $P_{\text{FPT}}(t) \propto t^{-3/2} \exp[-(at+2)^2/4Dt]$, where the heavy-tailed $t^{-3/2}$ prefactor reflects broad filament relaxation times [24].

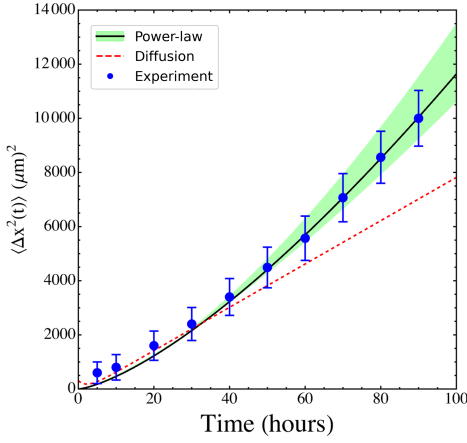


FIG. 2. Time evolution of the mean-squared displacement (MSD) for axons growing on PDMS micropatterns with $d = 3 \mu\text{m}$. Blue dots: MSD extracted from time-lapse fluorescence trajectories ($N \approx 90$ axons). Error bars indicate the standard error of the mean. Red dotted line: pure-diffusion prediction calculated with the experimentally determined diffusion coefficient $D = 20 \mu\text{m}^2 \text{h}^{-1}$. Black solid line: clutch-based stochastic model with exponent $\alpha = -0.6$, yielding $\langle x^2(t) \rangle \propto t^{2+\alpha} = t^{1.4}$. The surrounding narrow green band shows the model response for $-0.5 \leq \alpha \leq -0.7$, visualizing the sensitivity of the long-time scaling to variations in the power-law exponent.

During a fixed observation window the axon contains a renewing ensemble of N stochastically nucleated filaments. Linear response of the traction force $F(t)$ to a single filament's load step implies that:

$$a(t) \propto F(t) = \sum_{i=1}^N f_i e^{-\lambda_i t} \Theta(t - t_i) \quad (13)$$

where each mode decays with a rate $\lambda_i \sim 1/\text{lifetime}_i$. If we assume that the set $\{\lambda_i\}$ in Equation (13) inherits its statistics from the FPT distribution, we can relate the probability density of rates via the mapping $p(\lambda) d\lambda = R_{\text{FPT}}(t) dt$, with $t = 1/\lambda$. This yields a rate distribution with a tail that behaves as $p(\lambda) \propto t^{1/2}$. When combined with the exact expression given by MaxEnt principle (Equation (6)) this leads to a power-law exponent $\alpha = -1/2$. Therefore, the value of α is determined by the $t^{-3/2}$ tail of the disassembly time distribution characteristic for active actin and microtubule filaments.

For $\alpha = -1/2$, Equation (12) predicts a MSD scaling as $\langle x^2(t) \rangle \propto t^{1.5}$, which is in excellent agreement with the experimentally observed power-law behavior $\langle x^2(t) \rangle \propto t^{1.4}$ measured using fluorescence imaging of axons growing on PDMS micropatterns [21]. This close match between the theoretical prediction and experiment provides strong support for the clutch-based stochastic model, in which transient adhesion events and the active dynamics of actin and microtubule filaments together govern axonal growth.

To link our theoretical framework to empirical data, we acquired time-lapse fluorescence images of axons extending along PDMS micropatterned grooves with pattern spatial period $d = 3 \mu\text{m}$ (Fig. 1(c)). Analysis of the ensemble of trajectories in the early-time window ($t < 30 \text{h}$) provides direct estimates of the diffusion (cell motility) coefficient and damping constant, yielding $D = 20 \mu\text{m}^2 \text{h}^{-1}$ and $\gamma = 0.1 \text{h}^{-1}$, in agreement with our previous studies of axonal growth on similar substrates [19–22]. The parameter γ captures the combined effects of cytoskeletal drag, membrane tension, and weak adhesion to the PDMS surface, while D sets the magnitude of passive fluctuations. Together they define the diffusive baseline $\langle x^2(t) \rangle = 2Dt$ and the crossover time $t_c \sim \gamma^{-1}$ beyond which active processes dominate. Fig. 2 contrasts this diffusion baseline (red dotted line) with the clutch-based stochastic model. The diffusive prediction matches the experimental MSD (blue dots) up to $t \approx 30 \text{h}$; thereafter the data depart from the linear trend and follow the power-law curve $\langle x^2(t) \rangle \propto t^{1.4}$ expected for $\alpha = -0.6$ (black solid line). The sharp crossover, captured without additional fitting, confirms that the measured D and γ establish the passive regime, whereas intermittent clutch engagements with heavy-tailed lifetimes drive the observed super-diffusive extension at longer times.

The narrow green band surrounding the black power-law curve in Fig. 2, illustrates the model's sensitivity to small variations of the exponent in the range $-0.5 \leq \alpha \leq -0.7$. Each boundary of the band corresponds to the MSD scaling $\langle x^2(t) \rangle \propto t^{2+\alpha}$ evaluated at the limiting exponents, with the central black line marking the nominal value $\alpha = -0.6$. The experimental points remain confined within this shaded band for $t > 30 \text{h}$, confirming that small changes in α leave the long-time behavior essentially unchanged while still positioned well above the purely diffusive baseline. This shaded region thus provides a quantitative measure of the robustness of the clutch-based prediction: even when the acceleration statistics deviate from the predictions of Equation (9), the superdiffusive regime persists and continues to capture the observed axonal trajectories.

We next analyze the velocity-autocorrelation function, which characterizes the time-dependent memory of the growth-cone dynamics. By integrating Equation (10) and using Equation (9), we find that in the long-time limit ($\tau \gg \gamma^{-1}$) the velocity correlation function follows a power-law (see Supplemental Material [23]):

$$C_v(\tau) \simeq \frac{\sigma_a^2}{\gamma^2} \tau^\alpha, \quad \alpha = -0.6, \quad (14)$$

showing that velocity fluctuations retain long-range correlations even as their overall magnitude is attenuated by the square of the relaxation time $1/\gamma$. Equation (14) is the direct analogue of Eq. (12) for velocities: it couples

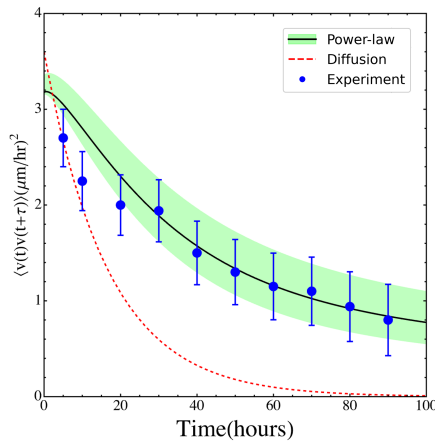


FIG. 3. Time dependence of the velocity-autocorrelation function $C_v(\tau)$ for axonal growth along $d = 3 \mu\text{m}$ PDMS micropatterns. Blue dots represent the experimental $C_v(\tau)$ obtained from the time-lapse imaging of the trajectories. Error bars indicate the standard error of the mean. Red dotted line: Ornstein-Uhlenbeck baseline $C_v(t) = 2D\gamma e^{-\gamma t}$ computed with the independently measured $D = 20 \mu\text{m}^2 \text{h}^{-1}$ and $\gamma = 0.1 \text{h}^{-1}$. Black solid line: clutch-based stochastic model with exponent $\alpha = -0.6$, giving the long-time power-law decay $C_v(t) \propto t^{-0.6}$. The narrow green band brackets the model response for $-0.5 \leq \alpha \leq -0.7$, demonstrating the robustness of the predicted scaling against variations in the power-law exponent.

the acceleration statistics to the exponential relaxation imposed by cytoskeletal damping and cell adhesion to the growth substrate. Fig. 3 compares this prediction (black curve, $\alpha = -0.6$) with the experimental $C_v(\tau)$ (blue dots) and with the purely diffusive OU baseline (red dotted line). A narrow green band, calculated for $-0.5 \leq \alpha \leq -0.7$, surrounds the theoretical curve, illustrating the robustness of the power-law decay: the data remain within this shaded region for $\tau > 30 \text{ h}$, confirming that small variations in adhesion statistics leave the long-time behavior essentially unchanged.

Discussion. Drawing on the Maximum Entropy (MaxEnt) principle, we have constructed the least-biased stochastic description that satisfies the experimentally accessible constraints on axonal traction forces. This method, rooted in Shannon-Jaynes formulation of entropy as a measure of missing information, has proven very powerful throughout statistical physics, from equilibrium ensembles to nonequilibrium steady states. By applying MaxEnt to the statistics of traction-force pulses, we derive a colored noise model that not only reproduces the observed anomalous scaling but also explains how heavy-tailed force fluctuations emerge from minimal dynamical assumptions. Our derivation pinpoints the disassembly statistics of active biopolymers and the clutch mechanism as the microscopic origins of the colored force noise that drives superdiffusive axonal growth.

The analytical form Eqs. (6), (12), and (14) also

yields direct, testable predictions. Inhibition of actin or microtubule dynamics (for example treatment with taxol or blebbistatin [19, 20, 22]), or ATP depletion should reduce the noise amplitude in the Langevin equation and delay the onset of superdiffusion. Moreover, pharmacological modulation of clutch unbinding rates will shift the exponent α and hence change both MSD and $C_v(\tau)$ scaling bands in Fig. 2 and Fig. 3. In future work we will measure the effects of such perturbations using the existing fluorescence-tracking protocol.

Beyond its immediate biological implications, our entropy-based inference offers a general framework for deriving coarse-grained dynamics in systems where mechanochemical details are underdetermined. The superdiffusive behavior uncovered in axonal motion aligns this biological system to a broad class of nonequilibrium processes characterized by long-range correlations and anomalous transport. Similar scaling laws appear in neural networks [9, 11, 12, 30], active colloids [5], Lévy walks [6, 31, 32], cellular migration [33], turbulent flows and glassy dynamics [34], suggesting that the power-law statistics observed here stem from universal physical principles rather than system-specific details. Isolating the minimal ingredients that generate such behavior is essential for building a predictive theory across these domains. By identifying the key ingredients of axonal growth, this work deepens our understanding of neuronal morphogenesis and advances a generalizable strategy for linking microscopic activity to emergent dynamics in active matter.

Acknowledgments. The authors gratefully acknowledge financial support for this work from National Science Foundation (DMR 2104294), Tufts Faculty Research Award (FRAC) (C.S.), and Tufts Summer Scholars Program (J.S.). We thank D.L. Kaplan and J.P. de Ruiter for stimulating discussions.

* cstaii01@tufts.edu

- [1] K. Franze and J. Guck, The biophysics of neuronal growth, *Reports on Progress in Physics* **73**, 094601 (2010).
- [2] L. A. Lowery and D. Van Vactor, The trip of the tip: understanding the growth cone machinery, *Nature Reviews Molecular Cell Biology* **10**, 332 (2009).
- [3] A. B. Huber, A. L. Kolodkin, D. D. Ginty, and J. F. Cloutier, Signaling at the growth cone: ligand-receptor complexes and the control of axon growth and guidance, *Annual Review of Neuroscience* **26**, 509 (2003).
- [4] P.-G. de Gennes, Collective neuronal growth and self organization of axons, *Proceedings of the National Academy of Sciences* **104**, 4904 (2007).
- [5] F. Peruani and L. G. Morelli, Self-propelled particles with fluctuating speed and direction of motion in two dimensions, *Phys. Rev. Lett.* **99**, 010602 (2007).
- [6] P. F. C. Tilles, S. V. Petrovskii, and P. L. Natti, A ran-

- dom acceleration model of individual animal movement allowing for diffusive, superdiffusive and superballistic regimes, *Scientific Reports* **7**, 14364 (2017).
- [7] H. Oliveri and A. Goriely, Mathematical models of neuronal growth, *Biomechanics and Modeling in Mechanobiology* **21**, 89 (2022).
 - [8] R. Alert and X. Trepac, Physical models of collective cell migration, *Annual Review of Condensed Matter Physics* **11**, 10.1146/annurev-conmatphys-031218-013516 (2020).
 - [9] G. Tkačik, O. Marre, T. Mora, D. Amodèi, M. J. Berry II, and W. Bialek, The simplest maximum entropy model for collective behavior in a neural network, *Journal of Statistical Mechanics: Theory and Experiment* **2013**, P03011 (2013).
 - [10] G. Amselem, M. Theves, A. Bae, E. Bodenschatz, and C. Beta, A stochastic description of dictyostelium chemotaxis, *PLoS One* **7**, e37213 (2012).
 - [11] Y. Song, D. Zhou, and S. Li, Maximum entropy principle underlies wiring length distribution in brain networks, *Cerebral Cortex* **31**, 4628 (2021).
 - [12] M. Lamberti, M. Hess, I. Dias, M. van Putten, J. le Feber, and S. Marzen, Maximum entropy models provide functional connectivity estimates in neural networks, *Scientific Reports* **12**, 9656 (2022).
 - [13] K. Franze, Integrating chemistry and mechanics: The forces driving axon growth, *Annual Review of Cell and Developmental Biology* **36**, 61 (2020).
 - [14] H. Oliveri, K. Franze, and A. Goriely, Theory for durotactic axon guidance, *Phys. Rev. Lett.* **126**, 118101 (2021).
 - [15] R. de Rooij, E. Kuhl, and K. E. Miller, Modeling the axon as an active partner with the growth cone in axonal elongation, *Biophysical Journal* **115**, 1783 (2018).
 - [16] A. Kundu, L. Micholt, S. Friedrich, D. R. Rand, C. Bartic, D. Braeken, and A. Levchenko, Superimposed topographic and chemical cues synergistically guide neurite outgrowth, *Lab on a Chip* **13**, 3070 (2013).
 - [17] M. Ishihara, N. Mochizuki-Oda, K. Iwatsuki, H. Kishima, Y. Iwamoto, Y. Ohnishi, M. Umegaki, and T. Yoshimine, A new three-dimensional axonal outgrowth assay for central nervous system regeneration, *Journal of Neuroscience Methods* **198**, 181 (2011).
 - [18] U. Kumarasinghe, L. N. Fox, and C. Staii, Combined traction force-atomic force microscopy measurements of neuronal cells, *Biomimetics* **7**, 10.3390/biomimetics7040157 (2022).
 - [19] J. M. Vensi Basso, I. Yurchenko, M. Simon, D. J. Rizzo, and C. Staii, Role of geometrical cues in neuronal growth, *Physical Review E* **99**, 022408 (2019).
 - [20] M. Descoteaux, J. P. Sunnerberg, D. D. Brady, and C. Staii, Feedback-controlled dynamics of neuronal cells on directional surfaces, *Biophysical Journal* **121**, 769 (2022).
 - [21] I. Yurchenko, J. M. Vensi Basso, V. S. Syrotenko, and C. Staii, Anomalous diffusion for neuronal growth on surfaces with controlled geometries, *PLoS One* **14**, e0216181 (2019).
 - [22] J. M. V. Basso, I. Yurchenko, M. R. Wiens, and C. Staii, Neuron dynamics on directional surfaces, *Soft Matter* **15**, 9931 (2019).
 - [23] See Supplemental Material at [URL], which includes Refs. [18-22], for experimental details, solution to the Maximum Entropy problem, and derivations for mean-square displacement and velocity autocorrelation functions.
 - [24] D. Swanson and N. S. Wingreen, Active biopolymers confer fast reorganization kinetics, *Phys. Rev. Lett.* **107**, 218103 (2011).
 - [25] K. Franze, J. Gerdemann, M. Weick, T. Betz, S. Pawlizak, M. Lakadamyali, J. Bayer, K. Rillich, M. Gögler, Y. B. Lu, A. Reichenbach, P. Janmey, and J. Käs, Neurite branch retraction is caused by a threshold-dependent mechanical impact, *Biophysical Journal* **97**, 1883 (2009).
 - [26] D. Koch, W. J. Rosoff, J. Jiang, H. M. Geller, and J. S. Urbach, Strength in the periphery: growth cone biomechanics and substrate rigidity response in peripheral and central nervous system neurons, *Biophysical Journal* **102**, 452 (2012).
 - [27] C. Hyland, A. F. Mertz, P. Forscher, and E. Dufresne, Dynamic peripheral traction forces balance stable neurite tension in regenerating aplasia bag cell neurons, *Scientific Reports* **4**, 4961 (2014).
 - [28] E. T. Jaynes, Information theory and statistical mechanics, *Phys. Rev.* **106**, 620 (1957).
 - [29] S. Pressé, K. Ghosh, J. Lee, and K. A. Dill, Principles of maximum entropy and maximum caliber in statistical physics, *Rev. Mod. Phys.* **85**, 1115 (2013).
 - [30] X.-Y. Zhang, J. M. Moore, X. Ru, and G. Yan, Geometric scaling law in real neuronal networks, *Phys. Rev. Lett.* **133**, 138401 (2024).
 - [31] A. M. Reynolds, Truncated lévy walks are expected beyond the scale of data collection when correlated random walks embody observed movement patterns, *J. R. Soc. Interface* **9**, 528 (2012).
 - [32] A. M. Edwards, R. A. Phillips, N. W. Watkins, M. P. Freeman, E. J. Murphy, V. Afanasyev, S. V. Buldyrev, M. G. E. da Luz, E. P. Raposo, H. E. Stanley, and G. M. Viswanathan, Revisiting lévy flight search patterns of wandering albatrosses, bumblebees and deer, *Nature* **449**, 1044 (2007).
 - [33] P. Dieterich, R. Klages, R. Preuss, and A. Schwab, Anomalous dynamics of cell migration, *Proc. Natl. Acad. Sci. U.S.A.* **105**, 459 (2008).
 - [34] R. Metzler and J. Klafter, The random walk's guide to anomalous diffusion: A fractional dynamics approach, *Phys. Rep.* **339**, 1 (2000).

Supplemental Material for Entropy-Constrained Noise Yields Superdiffusive Dynamics in Axonal Growth

This PDF file includes:

Experimental Details

Solution to the variational problem

Analysis of the power law dependence for the acceleration autocorrelation function

Analysis of the velocity autocorrelation function

EXPERIMENTAL DETAILS

Neuronal Cell Culture. Primary cortical neurons were obtained from embryonic day 18 rat embryos. All procedures involving animal tissue were approved by the Tufts University Institutional Animal Care and Use Committee and were conducted in accordance with NIH guidelines for the Care and Use of Laboratory Animals. Neuronal dissociation and culture were performed using established protocols described in our previous publications [18–22]. Briefly, cortices were incubated in 5 mL of trypsin at 37°C for 20 minutes. Enzymatic activity was subsequently inhibited by adding 10 mL of soybean trypsin inhibitor (Life Technologies). Neurons were then mechanically dissociated, centrifuged, and the supernatant was removed. The resulting cell pellet was resuspended in 20 mL of Neurobasal medium (Life Technologies) supplemented with GlutaMAX, b27 (Life Technologies), and penicillin-streptomycin. For fluorescence imaging, live cortical samples were rinsed once with phosphate-buffered saline (PBS), then incubated at 37°C for 30 minutes with 50 nM Tubulin Tracker Green (Oregon Green 488 Taxol, bis-Acetate, Life Technologies, Grand Island, NY) diluted in PBS. Following incubation, samples were rinsed twice with PBS and placed in fresh PBS for imaging. Fluorescence images were acquired using a standard FITC filter set (excitation/emission: 495 nm/521 nm), and axon outgrowth was quantified using the NeuronJ plugin for ImageJ. Immunostaining data from earlier studies confirmed high neuronal purity in these cultures. Cells were plated onto micropatterned polydimethylsiloxane (PDMS) substrates pre-coated with poly-D-lysine (PDL; 0.1 mg/mL, Sigma-Aldrich, St. Louis, MO) at a density of 4,000 cells/cm². As demonstrated in previous work, neuronal cultures maintained at low densities (3,000–7,000 cells/cm²) promote the development of long axons, making them well-suited for studying axonal dynamics under controlled surface cues [18–22].

Micropatterned Substrates. Micropatterns on the PDMS substrates consisted of parallel ridges separated by grooves (Figure 1 in the main text). These patterns were fabricated using a simple imprinting method in which diffraction gratings were pressed into uncured PDMS, producing periodic structures with a defined spatial period d . The PDL coating was applied via spin coating to ensure uniform surface treatment. Further details on substrate preparation and micropatterning techniques are provided in our previous publications [18–22].

Imaging and Data Acquisition. Atomic force microscopy (AFM) and fluorescence imaging were used to characterize both the substrates and neuronal growth. AFM images were acquired using an MFP-3D system (Asylum Research) equipped with a BioHeater fluid cell, integrated with an inverted Nikon Eclipse Ti microscope (Micro Video Instruments, Avon, MA). Fluorescence imaging of neurons was performed using standard FITC filters (excitation: 495 nm; emission: 521 nm).

Data Analysis. Growth cone dynamics were analyzed using ImageJ (NIH). The position of each growth cone was tracked by fluorescence microscopy, with images captured every $\Delta t = 5$ minutes over a total observation period of 30 minutes. Measurements were performed at multiple time points post-plating: $t = 10, 15, 20, 25, 30, 35, 40, 45$, and 50 hours. The chosen interval ($\Delta t = 5$ minutes) ensured that the displacement Δr of the growth cone exceeded the spatial resolution of the measurement (0.1 μm), and that the velocity estimate $\Delta r/\Delta t$ closely approximated the instantaneous growth velocity V . The growth angle θ was defined relative to the x -axis, as illustrated in Figure 1 in the main text.

SOLUTION OF THE VARIATIONAL PROBLEM

The goal is to determine the rate distribution $p(\lambda)$ ($\lambda > 0$) that maximises the Shannon–Jaynes entropy:

$$S[p] = - \int_0^\infty d\lambda \, p(\lambda) \ln \frac{p(\lambda)}{m(\lambda)}, \quad m(\lambda) = \lambda^{-1}, \quad (15)$$

subject to the constraints

$$\text{normalisation:} \quad \int_0^\infty p(\lambda) d\lambda = 1, \quad (16)$$

$$\text{finite mean relaxation rate:} \quad \int_0^\infty \lambda p(\lambda) d\lambda = \langle \lambda \rangle, \quad (17)$$

Introducing Lagrange multipliers α, β for the two constraints, and the Jeffreys prior $m(\lambda) = \lambda^{-(1+\alpha)}$ to promote exponentially decaying force pulses, we extremize the functional:

$$\mathcal{J}[p] = S[p] - \alpha \left(\int p - 1 \right) - \beta \left(\int \lambda p - \langle \lambda \rangle \right). \quad (18)$$

By varying $p \rightarrow p + \delta p$ with arbitrary $\delta p(\lambda)$, and using $\delta S = - \int \delta p \left[\ln \frac{p}{m} + 1 \right]$, the variation of Equation (18) is:

$$\delta \mathcal{J} = \int_0^\infty d\lambda \delta p(\lambda) \left[- \ln \frac{p(\lambda)}{m(\lambda)} - 1 - \alpha - \beta \lambda \right].$$

Because the bracket must vanish for every $p(\lambda)$:

$$\ln \frac{p(\lambda)}{m(\lambda)} = -1 - \alpha - \beta \lambda.$$

Substituting the prior $m(\lambda) = \lambda^{-(1+\alpha)}$ and solving for $p(\lambda)$ gives:

$$p(\lambda) = A \lambda^{(-1+\alpha)} e^{-\beta \lambda}, \quad A \equiv e^{-(1+\alpha)}. \quad (19)$$

or:

$$p(\lambda) = \frac{1}{Z} \lambda^{-(1+\alpha)} e^{-\beta \lambda}, \quad Z = \int_0^\infty \lambda^{-(1+\alpha)} e^{-\beta \lambda} d\lambda, \quad (20)$$

where we have absorbed A into the normalising constant Z .

We show that the normalization integral Z in Equation (20) reduces to the Gamma-like form:

$$Z = \beta^\alpha \Gamma(-\alpha).$$

The normalisation integral is:

$$Z = \int_0^\infty \lambda^{-(1+\alpha)} e^{-\beta \lambda} d\lambda.$$

Let $\rho \equiv -\alpha > 0$, then

$$Z = \int_0^\infty \lambda^{\rho-1} e^{-\beta \lambda} d\lambda.$$

Next, introduce the dimensionless variable $u = \beta \lambda$:

$$\lambda = \frac{u}{\beta}, \quad d\lambda = \frac{du}{\beta}.$$

Hence

$$Z = \int_0^\infty \left(\frac{u}{\beta} \right)^{\rho-1} e^{-u} \frac{du}{\beta} = \beta^{-\rho} \int_0^\infty u^{\rho-1} e^{-u} du.$$

By definition of the Gamma function, $\Gamma(\rho) = \int_0^\infty u^{\rho-1} e^{-u} du$ for $\rho > 0$. Therefore

$$Z = \beta^{-\rho} \Gamma(\rho) = \beta^\alpha \Gamma(-\alpha),$$

re-expressing $\rho = -\alpha$ in the final step. The conditions $\alpha < 0$ and $\beta > 0$ guarantee convergence at both integration limits.

The fixed mean $\langle \lambda \rangle$ determines the scale β :

$$\langle \lambda \rangle = \frac{1}{Z} \int_0^\infty \lambda^{-\alpha} e^{-\beta \lambda} d\lambda = \frac{\Gamma(1-\alpha)}{\beta \Gamma(-\alpha)} \implies \beta = \frac{\Gamma(1-\alpha)}{\langle \lambda \rangle \Gamma(-\alpha)}.$$

Note that all Lagrange multipliers are now fixed; no further structure can be added without violating the maximal-entropy condition.

ANALYSIS OF THE POWER LAW DEPENDENCE FOR THE ACCELERATION AUTOCORRELATION FUNCTION

We start with the stochastic Langevin equation:

$$\ddot{x}(t) = -\gamma \dot{x}(t) + a(t), \quad (21)$$

where $a(t)$ is a random acceleration with power-law autocorrelation:

$$\langle a(t) a(t + \tau) \rangle = \sigma_a^2 \tau^\alpha, \quad (22)$$

for $\tau > 0$, and $\gamma > 0$ is a damping constant. We wish to find the mean-square displacement $\langle x^2(t) \rangle$.

Solution for $x(t)$. First, rewrite (21) for the velocity $v(t) := \dot{x}(t)$:

$$\dot{v}(t) + \gamma v(t) = a(t),$$

Integrate to get the formal solution

$$v(t) = \int_0^t e^{-\gamma[t-s]} a(s) ds,$$

assuming zero initial velocity. Then

$$x(t) = \int_0^t v(u) du = \int_0^t \left[\int_0^u e^{-\gamma(u-s)} a(s) ds \right] du.$$

One can interchange integrals to obtain:

$$x(t) = \frac{1}{\gamma} \int_0^t \left[1 - e^{-\gamma[t-s]} \right] a(s) ds.$$

Expression for $\langle x^2(t) \rangle$ Since $x(t)$ is a linear functional of $a(s)$, we have

$$x(t) = \int_0^t f(t-s) a(s) ds, \quad \text{where} \quad f(\tau) = \frac{1}{\gamma} [1 - e^{-\gamma\tau}].$$

Then the mean-square displacement is

$$\begin{aligned} \langle x^2(t) \rangle &= \left\langle \int_0^t f(t-s) a(s) ds \times \int_0^t f(t-s') a(s') ds' \right\rangle \\ &= \int_0^t \int_0^t f(t-s) f(t-s') \langle a(s) a(s') \rangle ds ds'. \end{aligned}$$

Using the given correlation

$$\langle a(s) a(s') \rangle = \sigma_a^2 |s - s'|^\alpha,$$

we get

$$\langle x^2(t) \rangle = \sigma_a^2 \int_0^t \int_0^t f(t-s) f(t-s') |s - s'|^\alpha ds ds'. \quad (23)$$

Substituting $f(\tau) = \frac{1}{\gamma} [1 - e^{-\gamma\tau}]$, we find

$$\langle x^2(t) \rangle = \frac{\sigma_a^2}{\gamma^2} \int_0^t \int_0^t \left[1 - e^{-\gamma[t-s]} \right] \left[1 - e^{-\gamma[t-s']} \right] |s - s'|^\alpha ds ds'.$$

This double integral completely specifies the mean-square displacement at any finite t .

Large t asymptotics:

For times t large compared to $1/\gamma$, the exponentials $e^{-\gamma[t-s]}$ become negligible unless s is very close to t . Hence, for $t \gg 1/\gamma$, we can approximate

$$1 - e^{-\gamma[t-s]} \approx 1 \quad (\text{for most } 0 \leq s \ll t).$$

Thus,

$$\langle x^2(t) \rangle \approx \frac{\sigma_a^2}{\gamma^2} \int_0^t \int_0^t |s - s'|^\alpha ds ds'.$$

and the double integral becomes:

$$\int_0^t \int_0^t |s - s'|^\alpha ds ds' = 2 \int_0^t ds \int_0^s (s - s')^\alpha ds' = 2 \int_0^t \frac{s^{\alpha+1}}{\alpha+1} ds = 2 \frac{t^{\alpha+2}}{(\alpha+1)(\alpha+2)}.$$

Hence, for $t \gg 1/\gamma$,

$$\langle x^2(t) \rangle \sim \frac{2\sigma_a^2}{\gamma^2} \frac{t^{\alpha+2}}{(\alpha+1)(\alpha+2)}.$$

This power-law growth, $\langle x^2(t) \rangle \propto t^{\alpha+2}$, shows that the process may exhibit sub-, super-, or normal diffusion (and even super-ballistic) depending on the value of α .

Summary

Exact integral form:

$$\langle x^2(t) \rangle = \frac{\sigma_a^2}{\gamma^2} \int_0^t \int_0^t [1 - e^{-\gamma(t-s)}][1 - e^{-\gamma(t-s')}] |s - s'|^\alpha ds ds'.$$

Asymptotics for large t :

$$\langle x^2(t) \rangle \sim \frac{2\sigma_a^2}{\gamma^2 (\alpha+1)(\alpha+2)} t^{\alpha+2}.$$

ANALYSIS OF THEE VELOCITY AUTOCORRELATION FUNCTION

From Eq. (21),

$$v(t) = \dot{x}(t) = \int_0^t e^{-\gamma[t-s]} a(s) ds,$$

assuming $v(0) = 0$. We want to calculate $\langle v(t) v(t+\tau) \rangle$. Thus,

$$\begin{aligned} \langle v(t) v(t+\tau) \rangle &= \left\langle \int_0^t e^{-\gamma(t-s)} a(s) ds \times \int_0^{t+\tau} e^{-\gamma[(t+\tau)-s']} a(s') ds' \right\rangle \\ &= \int_0^t \int_0^{t+\tau} e^{-\gamma(t-s)} e^{-\gamma[(t+\tau)-s']} \langle a(s) a(s') \rangle ds ds'. \end{aligned}$$

Using $\langle a(s) a(s') \rangle = \sigma_a^2 |s - s'|^\alpha$, we get

$$\langle v(t) v(t+\tau) \rangle = \sigma_a^2 \int_0^t \int_0^{t+\tau} e^{-\gamma(t-s)} e^{-\gamma[(t+\tau)-s']} |s - s'|^\alpha ds ds'. \quad (24)$$

This is the velocity autocorrelation for the finite-time (non-stationary, i.e. axons growing) case.

Long t limit: In this limit, define the stationary autocorrelation function

$$C_v(\tau) = \lim_{\tau \rightarrow \infty} \langle v(t) v(t + \tau) \rangle.$$

The resulting integral typically depends on α in a nontrivial way, and closed-form solutions are only expressible in terms of special functions.

Asymptotic Evaluation of the Velocity Autocorrelation Function $C_v(\tau)$

In Equation (24) define:

$$x = t - s, \quad y = t + \tau - s', \quad (25)$$

Equation (24) becomes:

$$C_v^{(t)}(\tau) = \sigma_a^2 \int_0^t dx \int_0^{t+\tau} dy e^{-\gamma(x+y)} |\tau + x - y|^\alpha. \quad (26)$$

For $\tau \ll \gamma^{-1}$ we have:

$$C_v(\tau) \simeq \sigma_a^2 \tau^\alpha \left[\int_0^t dx e^{-\gamma x} \right] \left[\int_0^{t+\tau} dy e^{-\gamma y} \right]. \quad (27)$$

The integrals in Eq.(27) evaluate to:

$$\int_0^t dx e^{-\gamma x} = \frac{1 - e^{-\gamma t}}{\gamma}, \quad \int_0^{t+\tau} dy e^{-\gamma y} = \frac{1 - e^{-\gamma(t+\tau)}}{\gamma}. \quad (28)$$

and substitution back into Eq.(27) gives:

$$C_v(\tau) = \sigma_a^2 \tau^\alpha \frac{[1 - e^{-\gamma t}][1 - e^{-\gamma(t+\tau)}]}{\gamma^2}. \quad (29)$$

which in the limit ($t \gg \gamma^{-1}$) reduces to:

$$C_v(\tau) \simeq \frac{\sigma_a^2}{\gamma^2} \tau^\alpha. \quad (30)$$

as claimed in Equation (15) in the main text.